Time correlators from deferred measurements

D. Oehri,[1] A. V. Lebedev,[1] G. B. Lesovik,[2] and G. Blatter[1]
[1]*Theoretische Physik, ETH Zurich, CH-8093 Zurich, Switzerland*
[2]*L. D. Landau Institute for Theoretical Physics, RAS, 142432 Chernogolovka, Russia*
(Received 10 February 2015; revised manuscript received 18 November 2015; published 19 January 2016)

Repeated measurements that typically occur in two-time or multitime correlators rely on von Neumann's projection postulate, telling how to restart the system after an intermediate measurement. We invoke the principle of deferred measurement to describe an alternative procedure in which coevolving quantum memories extract system information through entanglement, combined with a final readout of the memories described by Born's rule. Our approach to repeated quantum measurements respects the unitary evolution of quantum mechanics during intermediate times, unifies the treatment of strong and weak measurements, and reproduces the projected and (anti)symmetrized correlators in the two limits. As an illustration, we apply our formalism to the calculation of the electron charge correlator in a mesoscopic physics setting, where single electron pulses assume the role of flying memory qubits. We propose an experimental setup that reduces the measurement of the time correlator to the measurement of currents and noise, exploiting the (pulsed) injection of electrons to cope with the challenge of performing short-time measurements.

DOI: 10.1103/PhysRevB.93.045308

I. INTRODUCTION

Within the quantum world, the question of what quantities can be measured in an experiment is often a nontrivial one, e.g., measuring time correlators (with times τ_j) requires finding the correct ordering of operators. Concrete examples in mesoscopic physics and quantum optics are the measurements of charge correlators [1–4] or full counting statistics [5–7] and that of photon correlators [8,9]. The question is usually resolved by including the measurement apparatus in the description, and its internal workings decide upon the form of the measured correlator. Examples are the Ampèremeter, the double-dot detector, and the spin counter used in Refs. [1,3,5], or the different photodetectors introduced by Glauber and Mandel [10]. These detectors then act back on the system, thereby influencing the measurement outcome, i.e., the specific form of the correlator. For example, a weak measurement such as that used in Ref. [1] (see also Ref. [11]) leads to symmetrized $[\mathcal{R}S(\tau_1,\tau_2)]$ and antisymmetrized $[\mathcal{I}S(\tau_1,\tau_2)]$ correlators weighted with different detector response functions [2,12], while a strong measurement produces a projected correlator $S^P(\tau_1,\tau_2)$.

These different forms of measured correlators can be derived [13] by invoking the von Neumann projection postulate [14], which tells us how to restart the system after the first measurement at τ_1 (or after previous measurements at times $\tau_j < \tau_n$ in an nth-order correlator). The measurement with a weakly coupled detector can be treated perturbatively, with the von Neumann projection exerted on the detector and no backaction on the system [1]. In a strong measurement with a large system-detector coupling, the projection can be formally applied directly to the system, thereby producing a maximal backaction [13].

In this paper, we invoke the principle of deferred measurement [15] known from quantum information theory, where it can be used for quantum computing, and we apply it to the problem of repeated measurements, specifically of time correlators. We replace the von Neumann projection by entangling the measured system with coevolving quantum memories (see Fig. 1), thereby (effectively) expanding the Hilbert space of the total system in every measurement step. The desired correlator is then derived from a final measurement of all the quantum memories by invoking Born's rule [16]. Hence the entire system plus memories undergoes a unitary quantum evolution until the very end, where the Born rule takes us from the quantum to the classical world. Our scheme captures the cases of weak and strong measurement within a unique formalism by merely changing the degree of entanglement between the system and the quantum memory. In the limits of weak and strong entanglement, we reproduce the results previously derived via use of the projection postulate. No simple physical form for the time correlators has been found so far in the intermediate-coupling regime.

Describing a measurement by entangling the system with a detector and including a (dissipative) bath in the evolution of the density matrix is a concept that has been well developed

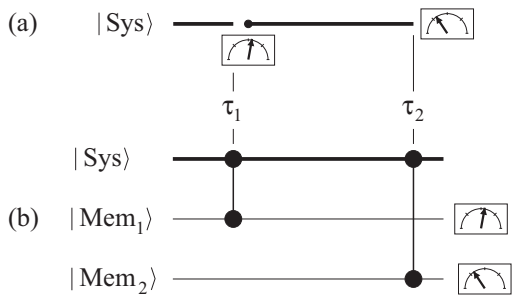

FIG. 1. Schematic illustration of different measurement procedures for a two-time ($\tau_1,\tau_2 > \tau_1$) correlator: (a) strong measurement described by von Neumann projection acting directly on the system at time τ_1 and providing a projected correlator S^P after readout at τ_2; for a weak measurement, the von Neumann projection at time τ_1 acts on the weakly coupled detector. (b) Repeated measurement without von Neumann projection at τ_1: unitary coevolution of the system and quantum memories that are entangled at times τ_1 and τ_2 and final readout after τ_2. The coupling strength between the system and the quantum memories determines the degree of entanglement.

over the past two decades [17–20]. Here, we extend the idea of system-detector entanglement to the case of repeated measurement. Thereby, the quantum memories evolve coherently during and after the information transfer from the system due to entanglement, with the (dissipative) measurement deferred to the very end of the process.

The proposed scheme for the measurement of time-correlated observables finds an interesting application in mesoscopic physics. In particular, measuring the charge $\hat{Q}$ dynamics of a quantum dot with the help of a nearby quantum point contact is a classic problem [21]. In such a setup, single-electron pulses [5,22] assume the role of flying qubit memories, which are either transmitted or reflected by the quantum point contact (QPC), depending on the dot's charge state; see Fig. 2. Analyzing the charge transmitted across the QPC then provides the desired information on the dot's charge correlator. Making use of recent developments in electron quantum optics [23,24], we propose a setup (see Fig. 3) that shifts the task of resolving short times, typically done on the level of the detection, to the proper timing of electron pulses and gate operations.

We briefly sketch the main idea of the paper: Consider a system observable $\hat{O}$ with an eigenbasis $\{|n\rangle\}$ that is to be measured. We start with a system state at the initial time $\tau_{\rm in}$,

$$|\psi(\tau_{\rm in})\rangle = \sum_n \psi_n(\tau_{\rm in})|n\rangle, \tag{1}$$

and a quantum memory in the initial state $|\phi^{(1)}_{\rm in}\rangle$, and we have them transiently interact at time τ_1 with the help of an externally controlled interaction (to be identified with a quantum detector). The system and memory then become entangled,

$$\left[\sum_n \psi_n(\tau_1)|n\rangle\right]\left|\phi^{(1)}_{\rm in}\right\rangle \to \sum_n \psi_n(\tau_1)|n\rangle\left|\phi^{(1)}_n\right\rangle, \tag{2}$$

where $|\phi^{(1)}_n\rangle$ denote memory states after interaction with the system in state $|n\rangle$, and we assume a negligible evolution of the system during the time of interaction. Evolving the system to the later time τ_2 and entangling it with a second memory, we obtain the state

$$\sum_{m,n} U_{mn}(\tau_{21})\psi_n(\tau_1)|m\rangle\left|\phi^{(1)}_n\right\rangle\left|\phi^{(2)}_m\right\rangle, \tag{3}$$

with $U_{mn}(\tau)$ the matrix elements of the system propagator $\hat{U}(\tau)$ and $\tau_{21} = \tau_2 - \tau_1$. The unitary evolution of the memory states $|\phi^{(j)}_n\rangle$ preserves the system information gained at times τ_j. At time $\tau_{\rm fin} > \tau_2$, we measure the memory observables $\hat{a}^{(1)}$ and $\hat{a}^{(2)}$ with discrete spectra $a^{(1,2)}_\alpha$. Making use of Born's rule, we find the probability distribution function $P_{\alpha\beta}$ for the measurement outcomes α and β on the two memory observables; this probability distribution contains the desired information on the system's two-time correlator. The specific relation between the distribution function $P_{\alpha\beta}$ of measurement outcomes and the correlator of system observables $\hat{O}(\tau_1)$ and $\hat{O}(\tau_2)$ depends on the system-detector coupling and the observables measured on the memories; we will show below how to extract the well-known (anti)symmetrized and projected correlators from the probabilities $P_{\alpha\beta}$ in the limits of weak and strong measurements.

In the end, by making use of quantum memories that store the information acquired from the system at the quantum level at earlier times τ_1 and τ_2 until the final time $\tau_{\rm fin}$, we have avoided the intermediate readout, which requires the use of the projection postulate. Hence the entire measurement process follows a unitary quantum evolution until the transition to the classical world is done via Born's rule.

In the following, we will first derive the general framework describing the deferred measurement of a correlator with the intermediate von Neumann projection replaced by a system-detector entanglement (Sec. II). In Sec. II A, we discuss the limit of weak measurement, and we use qubits as quantum memories to arrive at a simple relation between the measurement outcome on the qubits and the (anti)symmetrized correlators of the system. In Sec. II B, we first discuss a strong measurement at strong coupling using qudit memories, and then we invoke (weakly coupled) qubit registers to show that both types of strong measurements produce the projected time correlator of the system. An illustration of our formalism is given in Sec. III, where we describe the measurement of the charge correlator in a mesoscopic setting, specifically the two-time charge correlator of a quantum dot (QD) as measured by a quantum point contact (QPC). Section III E describes a possible experimental implementation, and in Sec. IV we summarize our results.

II. CORRELATOR MEASUREMENTS BY QUANTUM MEMORIES

We consider the situation in which a two-time correlator of a system operator $\hat{O}$ is measured with the help of two quantum memories; the system's initial state $|\psi\rangle$ is given by Eq. (1), while the memories are described by initial states $|\phi^{(j)}_{\rm in}\rangle$, $j = 1,2$ (see below for the discussion of an open system described by a density matrix $\hat{\rho}$). The memories interact with the system at times $\tau_{1,2}$ during a small time interval $\delta\tau$. After this interaction, the resulting memory states $|\phi^{(j)}_n\rangle = \hat{u}_n|\phi^{(j)}_{\rm in}\rangle$ depend on the system state $|n\rangle$, where $\hat{u}_n$ describes the time evolution of the quantum memories during the interaction with the system (we assume a trivial evolution of the free memories). The system state $|\psi(\tau)\rangle = \sum_n \psi_n(\tau)|n\rangle$ is assumed to remain unchanged during the time $\delta\tau$ of the individual interaction events; see Sec. III C for an extended discussion of this point. After the second interaction event at τ_2, the wave function $|\psi(\tau_{\rm fin} > \tau_2)\rangle$ of the system is entangled with the states $|\phi^{(j)}_n\rangle$ of the memories, and the combined wave function $|\Psi_f\rangle$ reads

$$|\Psi_f\rangle = \sum_{l,m,n} U_{lm}(\tau_{f2})U_{mn}(\tau_{21})\psi_n(\tau_1)\,|l\rangle\left|\phi^{(1)}_n\right\rangle\left|\phi^{(2)}_m\right\rangle, \tag{4}$$

with $\tau_{f2} = \tau_{\rm fin} - \tau_2$. The quantum memories are supposed to retain their system information after their interaction. At time $\tau_{\rm fin}$, we measure the operators $\hat{a}^{(1)}$ and $\hat{a}^{(2)}$ on the first and second memory, respectively. Denoting the (discrete) eigenvalues and eigenstates of $\hat{a}^{(j)}$ by $a^{(j)}_\alpha$ and $|\varphi^{(j)}_\alpha\rangle$, we rewrite the memory states $|\phi^{(j)}_n\rangle = \sum_\alpha s^\alpha_n|\varphi^{(j)}_\alpha\rangle$. Applying Born's rule to the final state (4) provides us with the probability distribution

$$P_{\alpha\beta}(\tau_{21}) = \langle\Psi_f|\hat{p}^{(1)}_\alpha\hat{p}^{(2)}_\beta|\Psi_f\rangle, \tag{5}$$

where $\hat{p}_\alpha^{(j)}$ is the projector onto the eigenstate α of the jth memory, i.e., $\hat{p}_\alpha^{(j)} = |\varphi_\alpha^{(j)}\rangle\langle\varphi_\alpha^{(j)}|$. Making use of the unitarity condition $\sum_l U_{lm}U^*_{lm'} = \delta_{mm'}$ [rendering the evolution $U_{lm}(\tau_{f2})$ in Eq. (4) irrelevant], we obtain the probabilities

$$P_{\alpha\beta}(\tau_{21}) = \sum_m \left| \sum_n s_m^\beta U_{mn}(\tau_{21}) s_n^\alpha \psi_n(\tau_1) \right|^2. \tag{6}$$

The above expressions (5) and (6) for the probabilities $P_{\alpha\beta}(\tau_{21})$ provide us with the desired information on the two-time correlator of the system. They are easily generalized to the case of open systems by introducing the combined system plus bath (the open system) density matrix $\hat{\rho}$, and evolving it in time including the subsequent entanglement with the quantum memories: Starting from the initial density matrix $\hat{\rho}_0 \otimes |\phi_{\rm in}^{(1)}\rangle\langle\phi_{\rm in}^{(1)}| \otimes |\phi_{\rm in}^{(2)}\rangle\langle\phi_{\rm in}^{(2)}|$ describing the open system plus memories at time $\tau_{\rm in}$, we proceed as in the case of isolated systems by conditioning the time evolution of the memory states on the corresponding system states, and we obtain the final density matrix at time τ_f,

$$\hat{\rho}_f = \sum_{k,k',n,n',m,m} \hat{U}_{km}(\tau_{f2})\hat{U}_{mn}(\tau_{21})\,\hat{\rho}_{nn'}(\tau_1)\,\hat{U}^\dagger_{n'm'}(\tau_{21}) \times \hat{U}^\dagger_{m'k'}(\tau_{f2})\,|k\rangle\langle k'| \otimes \left|\phi_n^{(1)}\right\rangle\!\left\langle\phi_{n'}^{(1)}\right| \otimes \left|\phi_m^{(2)}\right\rangle\!\left\langle\phi_{m'}^{(2)}\right|, \tag{7}$$

with the open system's density matrix $\hat{\rho}(\tau_1)$ at time τ_1, its reduced part $\hat{\rho}_{nn'}(\tau_1) = \langle n|\hat{\rho}|n'\rangle$, and the reduced operators $\hat{U}_{il} = \langle i|\hat{U}|l\rangle$, with $\hat{U}$ the evolution operator of the open system. Note that here, the outgoing states $|\phi_{n^{(\prime)}}^{(1)}\rangle$ and $|\phi_{m^{(\prime)}}^{(2)}\rangle$ are conditioned on the system states $n^{(\prime)}$ and $m^{(\prime)}$ at times τ_1 and τ_2. We define the probabilities $P_{\alpha\beta}$ as

$$P_{\alpha\beta}(\tau_{21}) = \mathrm{Tr}\big[\hat{p}_\alpha^{(1)}\hat{p}_\beta^{(2)}\hat{\rho}_f\big] \tag{8}$$

with the trace taken over both the open system and the memory states. Calculating this expression with the final density matrix Eq. (7), we obtain

$$P_{\alpha\beta}(\tau_{21}) = \sum_{n,n',m} \mathrm{Tr}\big[s_m^\beta\,\hat{U}_{mn}(\tau_{21})\,s_n^\alpha\,\hat{\rho}_{nn'}(\tau_1)s_{n'}^{\alpha*}\,\hat{U}^\dagger_{n'm}(\tau_{21})\,s_m^{\beta*}\big], \tag{9}$$

with the remaining trace taken over the bath degrees of freedom. This result is the direct generalization of (6) to the case of open systems. Expressions (5) and (6) as well as (8) and (9) constitute the basic formulas, which we will develop further in the following sections. Indeed, as expressed in terms of the evolution amplitudes of the system and detectors, it is difficult to appreciate the physical meaning and content of these results. To make progress, we consider next the two cases of weak and strong measurements.

A. Weak measurement

Given a *weak system-detector coupling*, the most direct way to find the probabilities $P_{\alpha\beta}$ in terms of physically transparent quantities is to start from Eq. (5) and evaluate this expression perturbatively in the linear system-detector coupling $H_{\rm sd} = \sum_j \hat{b}^{(j)}(\tau)\hat{O}$, where the time-dependent coupling $\hat{b}^{(j)}(\tau)$ acts on the jth memory during a time $\delta\tau$ around τ_j. The unperturbed evolution of the memories is described by the Hamiltonian $\hat{h}_0$, and we make use of the interaction representation. We go over to irreducible quantities by subtracting the uncorrelated contribution,

$$P^{\rm irr}_{\alpha\beta} = P_{\alpha\beta} - P^{(1)}_\alpha P^{(2)}_\beta, \tag{10}$$

with $P^{(1)}_\alpha = \langle\Psi_f^{(1)}|\hat{p}_\alpha^{(1)}|\Psi_f^{(1)}\rangle$ and $P^{(2)}_\beta = \langle\Psi_f^{(2)}|\hat{p}_\beta^{(2)}|\Psi_f^{(2)}\rangle$ describing measurements involving a single entanglement at time τ_1 or τ_2 with only one memory, respectively. The quantity $P^{(1)}_\alpha$ can be obtained by a simple summation of $P_{\alpha\beta}$,

$$P^{(1)}_\alpha = \sum_\beta P_{\alpha\beta}, \tag{11}$$

and $P^{(2)}_\alpha = P^{(1)}_\alpha$ for a time-independent problem (otherwise, the determination of $P^{(2)}_\alpha$ necessitates a second measurement). Note that the sum over the first index of $P_{\alpha\beta}$ already includes correlations [see Eq. (6)], and hence $P^{(2)}_\beta \neq \sum_\alpha P_{\alpha\beta}$.

The task then is to evaluate the irreducible expression

$$P^{\rm irr}_{\alpha\beta} = \langle\!\langle\Psi|\hat{U}_D^\dagger(\tau_f,\tau_{\rm in})\hat{p}^{(1)}_\alpha(\tau_f)\hat{p}^{(2)}_\beta(\tau_f)\hat{U}_D(\tau_f,\tau_{\rm in})|\Psi\rangle\!\rangle, \tag{12}$$

with the expectation value to be taken over the initial system state $|\psi(\tau_{\rm in})\rangle$, $\langle\!\langle\cdot\rangle\!\rangle$ refers to the irreducible part, and the time evolution operator reads

$$\hat{U}_D(\tau_f,\tau_{\rm in}) = \mathcal{T}\exp\left[-\frac{i}{\hbar}\int_{\tau_{\rm in}}^{\tau_f} d\tau'\hat{H}_{\rm sd}(\tau')\right], \tag{13}$$

with $\mathcal{T}$ denoting time-ordering. Evaluating (12) to lowest relevant order in the coupling, we find

$$\begin{aligned}
P^{\rm irr}_{\alpha\beta} &= \frac{(-i)^2}{\hbar^2}\int_{\tau_{\rm in}}^{\tau_f} d\tau' \int_{\tau_{\rm in}}^{\tau'} d\tau''\,\langle\!\langle\Psi|\Big[\Big[\hat{p}^{(1)}_\alpha(\tau_f)\hat{p}^{(2)}_\beta(\tau_f),\hat{H}_{\rm sd}(\tau')\Big],\hat{H}_{\rm sd}(\tau'')\Big]|\Psi\rangle\!\rangle \\
&= \frac{(-i)^2}{\hbar^2}\int_{\tau_{\rm in}}^{\tau} d\tau' \int_{\tau_{\rm in}}^{\tau'} d\tau''\Big[\langle\!\langle\psi|\hat{O}(\tau')\hat{O}(\tau'')|\psi\rangle\!\rangle\,\big\langle\phi_{\rm in}^{(1)}\big|\hat{p}^{(1)}_\alpha(\tau_f)\hat{b}^{(1)}(\tau'')\big|\phi_{\rm in}^{(1)}\big\rangle\big\langle\phi_{\rm in}^{(2)}\big|\hat{p}^{(2)}_\beta(\tau_f)\hat{b}^{(2)}(\tau')\big|\phi_{\rm in}^{(2)}\big\rangle \\
&\quad - \langle\!\langle\psi|\hat{O}(\tau'')\hat{O}(\tau')|\psi\rangle\!\rangle\,\big\langle\phi_{\rm in}^{(1)}\big|\hat{b}^{(1)}(\tau'')\hat{p}^{(1)}_\alpha(\tau_f)\big|\phi_{\rm in}^{(1)}\big\rangle\big\langle\phi_{\rm in}^{(2)}\big|\hat{p}^{(2)}_\beta(\tau_f)\hat{b}^{(2)}(\tau')\big|\phi_{\rm in}^{(2)}\big\rangle \\
&\quad - \langle\!\langle\psi|\hat{O}(\tau')\hat{O}(\tau'')|\psi\rangle\!\rangle\,\big\langle\phi_{\rm in}^{(1)}\big|\hat{p}^{(1)}_\alpha(\tau_f)\hat{b}^{(1)}(\tau'')\big|\phi_{\rm in}^{(1)}\big\rangle\big\langle\phi_{\rm in}^{(2)}\big|\hat{b}^{(2)}(\tau')\hat{p}^{(2)}_\beta(\tau_f)\big|\phi_{\rm in}^{(2)}\big\rangle \\
&\quad + \langle\!\langle\psi|\hat{O}(\tau'')\hat{O}(\tau')|\psi\rangle\!\rangle\,\big\langle\phi_{\rm in}^{(1)}\big|\hat{b}^{(1)}(\tau'')\hat{p}^{(1)}_\alpha(\tau_f)\big|\phi_{\rm in}^{(1)}\big\rangle\big\langle\phi_{\rm in}^{(2)}\big|\hat{b}^{(2)}(\tau')\hat{p}^{(2)}_\beta(\tau_f)\big|\phi_{\rm in}^{(2)}\big\rangle\Big],
\end{aligned} \tag{14}$$

where we made sure that the first memory interacts with the system at the earlier time τ''. For a slow system dynamics and exploiting that $\hat{b}^{(j)}(\tau)|\phi_{\rm in}^{(j)}\rangle \neq 0$ only for $\tau \approx \tau_j$, we can replace $\hat{O}(\tau'') \to \hat{O}(\tau_1)$ and $\hat{O}(\tau') \to \hat{O}(\tau_2)$. We make use of the

standard definitions for the symmetrized and antisymmetrized irreducible correlators (with $[\cdot,\cdot]$ and $\{\cdot,\cdot\}$ denoting the usual commutator and anticommutator),

$$\mathcal{R}S^{\rm irr}_{OO}(\tau_1,\tau_2) = \langle\langle\{\hat{O}(\tau_1),\hat{O}(\tau_2)\}\rangle\rangle/2, \tag{15}$$

$$\mathcal{I}S^{\rm irr}_{OO}(\tau_1,\tau_2) = -i\langle\langle[\hat{O}(\tau_1),\hat{O}(\tau_2)]\rangle\rangle, \tag{16}$$

to arrive at the final result,

$$\begin{aligned} P^{\rm irr}_{\alpha\beta}(\tau_{21}) =& \mathcal{I}S^{(1)}_{{\rm det},\alpha}\mathcal{I}S^{(2)}_{{\rm det},\beta}\mathcal{R}S^{\rm irr}_{OO}(\tau_1,\tau_2) \\ &+ \mathcal{R}S^{(1)}_{{\rm det},\alpha}\mathcal{I}S^{(2)}_{{\rm det},\beta}\mathcal{I}S^{\rm irr}_{OO}(\tau_1,\tau_2), \end{aligned} \tag{17}$$

with the detector response functions

$$\mathcal{R}S^{(j)}_{{\rm det},\alpha} = -\frac{1}{2\hbar}\int_{\tau_{\rm in}}^{\tau_f} d\tau\langle\phi^{(j)}_{\rm in}|\{\hat{p}^{(j)}_\alpha(\tau_f),\hat{b}(\tau)\}|\phi^{(j)}_{\rm in}\rangle, \tag{18}$$

$$\mathcal{I}S^{(j)}_{{\rm det},\alpha} = \frac{-i}{\hbar}\int_{\tau_{\rm in}}^{\tau_f} d\tau\langle\phi^{(j)}_{\rm in}|[\hat{p}^{(j)}_\alpha(\tau_f),\hat{b}(\tau)]|\phi^{(j)}_{\rm in}\rangle. \tag{19}$$

The symbols $\mathcal{R}$ and $\mathcal{I}$ address symmetrized and antisymmetrized quantities (or equivalently, up to factors of 2, real and imaginary parts).

In a situation in which the full information $P_{\alpha\beta}$ can be extracted from the memories, the individual correlators $\mathcal{R}S^{\rm irr}_{OO}$ and $\mathcal{I}S^{\rm irr}_{OO}$ can be obtained from (17) by combining two different probabilities, e.g., using $P^{\rm irr}_{\alpha\beta}$ and $P^{\rm irr}_{\bar\alpha\beta}$ one obtains

$$\mathcal{R}S^{\rm irr}_{OO} = \left[\mathcal{R}S^{(1)}_{{\rm det},\bar\alpha}P^{\rm irr}_{\alpha\beta} - \mathcal{R}S^{(1)}_{{\rm det},\alpha}P^{\rm irr}_{\bar\alpha\beta}\right]/D^{(1)}\,\mathcal{I}S^{(2)}_{{\rm det},\beta}, \tag{20}$$

$$\mathcal{I}S^{\rm irr}_{OO} = \left[-\mathcal{I}S^{(1)}_{{\rm det},\bar\alpha}P^{\rm irr}_{\alpha\beta} + \mathcal{I}S^{(1)}_{{\rm det},\alpha}P^{\rm irr}_{\bar\alpha\beta}\right]/D^{(1)}\,\mathcal{I}S^{(2)}_{{\rm det},\beta}, \tag{21}$$

with $D^{(1)} = \mathcal{R}S^{(1)}_{{\rm det},\bar\alpha}\mathcal{I}S^{(1)}_{{\rm det},\alpha} - \mathcal{R}S^{(1)}_{{\rm det},\alpha}\mathcal{I}S^{(1)}_{{\rm det},\bar\alpha}$. Alternatively, one may have preferential access to combinations of probabilities $P_{\alpha\beta}$ (see Sec. III E for an example) or make use of specific detector properties; see below and the Appendix for examples.

A generic choice for the quantum memories are qubit devices that couple to the system via the Hamiltonian $\hat{H}_{\rm sd}(\tau) = \Omega(\tau)\hat{\sigma}_x\hat{O}$, where the coupling $\Omega(\tau)$ is switched on during a short time $\delta\tau$ around τ_j. Assuming initial states

$$|\phi^{(j)}_{\rm in}\rangle = [|\varphi_0\rangle + e^{i\theta^{(j)}}|\varphi_1\rangle]/\sqrt{2}, \tag{22}$$

a system residing in a state $|n\rangle$ with eigenvalue O_n will rotate the qubit around the x axis by $\delta\vartheta\ O_n$ with $\delta\vartheta = \Omega\delta\tau/\hbar$. The response functions (18) and (19) involve integrals of the type

$$\int_{\tau_{\rm in}}^{\tau_f} d\tau\langle\phi^{(j)}_{\rm in}|\hat{p}_\alpha(\tau_f)\Omega(\tau)\hat{\sigma}_x|\phi^{(j)}_{\rm in}\rangle = \delta\vartheta\ e^{i(1-2\alpha)\theta^{(j)}}, \tag{23}$$

and we obtain the response functions

$$\mathcal{R}S^{(j)}_{{\rm det},0} = \delta\vartheta\ \cos\theta^{(j)}, \quad \mathcal{R}S^{(j)}_{{\rm det},1} = \delta\vartheta\ \cos\theta^{(j)}, \tag{24}$$

$$\mathcal{I}S^{(j)}_{{\rm det},0} = 2\delta\vartheta\ \sin\theta^{(j)}, \quad \mathcal{I}S^{(j)}_{{\rm det},1} = -2\delta\vartheta\ \sin\theta^{(j)}. \tag{25}$$

Choosing $\theta^{(2)} = \pi/2$, i.e., polarizing the second memory along the y axis, we can directly find the correlator $\mathcal{R}S^{\rm irr}_{OO}$ ($\mathcal{I}S^{\rm irr}_{OO}$) from the memory correlator $P^{\rm irr}_{\alpha\beta}$ by choosing $\theta^{(1)} = \pi/2$ ($\theta^{(1)} = 0$). Alternatively, we may use the results (20) and (21) and $\theta^{(1)} = \theta^{(2)} = \pi/4$ to find (we choose $\alpha = 0$, $\bar\alpha = 1$, and $\beta = 0$)

$$\mathcal{R}S^{\rm irr}_{OO} = \frac{P^{\rm irr}_{00} - P^{\rm irr}_{10}}{4\delta\vartheta^2}, \tag{26}$$

$$\mathcal{I}S^{\rm irr}_{OO} = -\frac{P^{\rm irr}_{00} + P^{\rm irr}_{10}}{2\delta\vartheta^2}. \tag{27}$$

Note that the sums $P^{\rm irr}_{00} + P^{\rm irr}_{10}$ and $P^{\rm irr}_{00} + P^{\rm irr}_{01}$ contain very different types of information, one a correlation and the other only a mean value, as discussed in more detail in Sec. III E. Hence, we find that the delayed measurement of the two quantum memories provides the symmetrized and antisymmetrized correlators (15) and (16). Finally, we note that a weak linear coupling between the system observable and the detector/memory variable canonically conjugated to the detector readout provides a more effective entanglement. Such a von Neumann–like interaction allows to produce a strong entanglement and a strong measurement even for weak coupling if sufficient time is available for the entanglement process [25].

B. Strong measurement

We are now going to show that a *strong system-detector coupling* naturally leads to projective correlators. Consider a situation in which the system operator $\hat{O}$ is measured via entanglement with two quantum memories. We first consider an operator $\hat{O}$ with a nondegenerate spectrum, and we comment on the general case in the end. A strong coupling between the system and the memory implies that the memory states $|\phi^{(j)}_n\rangle$ after interaction with the system in state $|n\rangle$ are fully distinguishable, i.e.,

$$\langle\phi^{(j)}_m|\phi^{(j)}_n\rangle = \delta_{nm}. \tag{28}$$

The observables $\hat{a}^{(j)}$ distinguish between memory eigenstates $|\varphi^{(j)}_\alpha\rangle$, and we assume a one-to-one relation with the evoluted memory states $|\phi^{(j)}_n\rangle$,

$$|\phi^{(j)}_n\rangle = |\varphi^{(j)}_{\alpha_n}\rangle, \tag{29}$$

with $\alpha_n \neq \alpha_m$ for $n \neq m$ (otherwise, the observable $\hat{a}^{(j)}$ measures linear combinations of eigenstates of $\hat{O}$ and thus is not suitable for a measurement of this observable). Under these (strong-coupling) conditions, the amplitudes s^α_n reduce to $s^\alpha_n = \delta_{\alpha\alpha_n}$ (for $j = 1$, $s^\beta_m = \delta_{\beta\beta_m}$ for the second memory). To describe the strong-coupling situation, it is favorable to proceed with the expression (6), and we obtain the result

$$P_{\alpha_n\beta_m}(\tau_{21}) = |U_{mn}(\tau_{21})\psi_n(\tau_1)|^2. \tag{30}$$

The right-hand side of the above expression is merely the projected system correlator

$$\begin{aligned} S^P_{P_nP_m}(\tau_{21}) &= \sum_l \langle l|\hat{P}_m(\tau_2)\hat{P}_n(\tau_1)\rho_0\hat{P}_n(\tau_1)|l\rangle \\ &= |U_{mn}(\tau_{21})\psi_n(\tau_1)|^2, \end{aligned} \tag{31}$$

with the projected density matrix $\rho^P(\tau_1) = \sum_k \hat{P}_k(\tau_1)\ \rho_0\hat{P}_k(\tau_1)$ and the projectors $\hat{P}_k = |k\rangle\langle k|$ onto different system states; see Eq. (1). The projected correlators $S^P_{P_nP_m}(\tau_{21})$ are easily combined into the desired two-time

correlator $S^P_{OO}(\tau_{21})$,

$$\begin{aligned} S^P_{OO}(\tau_{21}) &= \mathrm{Tr}[\hat{O}(\tau_2)\hat{O}(\tau_1)\rho^P(\tau_1)] \\ &= \sum_{nm} O_n O_m S^P_{P_n P_m}(\tau_{21}) \\ &= \sum_{nm} O_n O_m P_{\alpha_n\beta_m}(\tau_{21}), \end{aligned} \tag{32}$$

thereby establishing the general result relating the system correlator to the memory readings. A further simplification can be achieved if the eigenvalues of $\hat{a}^{(j)}$ and $\hat{O}$ obey a linear relation $O_n = \eta^{(j)} a^{(j)}_{\alpha_n}$, in which case we obtain the simple result

$$\begin{aligned} S^P_{OO}(\tau_{21}) &= \sum_{nm} \eta^{(1)} a^{(1)}_{\alpha_n} \eta^{(2)} a^{(2)}_{\beta_m} P_{\alpha_n\beta_m}(\tau_{21}) \\ &= \eta^{(1)}\eta^{(2)} \langle \hat{a}^{(1)}\hat{a}^{(2)}\rangle, \end{aligned} \tag{33}$$

directly relating the projected system correlator to the memory correlator $\langle \hat{a}^{(1)}\hat{a}^{(2)}\rangle$.

These results can easily be generalized to the case in which the observable $\hat{O}$ involves a degenerate spectrum: The system evolution of the memories is conditioned on the eigenvalue O_n rather than the state $|n\rangle$ of the system. Degenerate eigenstates produce equal evolutions of the memories, implying that $P_{\alpha_n\beta_m}(\tau_{21})$ has to be replaced by $P_{\alpha_O\beta_{O'}}(\tau_{21}) = \sum_{\{m|O_m=O'\}} |\sum_{\{n|O_n=O\}} U_{mn}(\tau_{21})\psi_n(\tau_1)|^2$ and $\rho^P(\tau_1)$ is substituted by $\sum_O \hat{P}_O(\tau_1)\rho_0\hat{P}_O(\tau_1)$ with the projection operator $\hat{P}_O = \sum_{\{n|O_n=O\}} |n\rangle\langle n|$. With these replacements, the above results remain valid also for a degenerate spectrum.

Hence, the perfect entanglement between the system and the memories arising due to strong coupling is equivalent to a von Neumann projection applied to the system. While no backaction is apparent on the level of the system dynamics, the strong backaction of this maximal entanglement with the memories manifests itself in a strong change of the system's density matrix when tracing over the memories.

The realization of a strong measurement as described above requires equal or more memory states $|\varphi_\alpha\rangle$ than system states $|n\rangle$, hence quantum memories with dimensionality d or qudits are required. Besides the obvious difficulty in realizing qudit memories, their coupling to the system in order to serve as a measurement device is equally nontrivial. As an alternative, we discuss a measurement scheme involving qubit registers.

Such an alternative setup implementing a strong measurement involves a weak system-detector coupling but invokes multiple measurements. We replace the strongly coupled qudit memories by weakly coupled qubit registers with J qubits each, probing the system state close to τ_1 and τ_2 within a short time interval $\delta\tau$. For a strong measurement, J is chosen sufficiently large to distinguish the different eigenvalues O_n of the system. Assuming the system does not change during the interaction time $J\delta\tau$ with one register, the final state of the system and memory registers is of the same form as in Eq. (4), with the outgoing individual memory states $|\phi^{(1)}_n\rangle$ and $|\phi^{(2)}_m\rangle$ replaced by the outgoing register states $|\Phi^{(1)}_n\rangle = \prod_{j=1}^J |\phi^{(j)}_n\rangle$ and $|\Phi^{(2)}_m\rangle = \prod_{j=J+1}^{2J} |\phi^{(j)}_m\rangle$. Making use of Born's rule, we obtain the probabilities $P^{\mu\nu}_{\alpha\beta}(\tau_{21})$ for finding μ (ν) qubits of the first (second) register in states $\alpha \in \{0,1\}$ ($\beta \in \{0,1\}$),

$$\begin{aligned} P^{\mu\nu}_{\alpha\beta} = \binom{J}{\mu}\binom{J}{\nu} \sum_m \Big| \sum_n \big(s^\beta_m\big)^\nu \big(s^{\bar\beta}_m\big)^{J-\nu} \\ \times U_{mn} \big(s^\alpha_n\big)^\mu \big(s^{\bar\alpha}_n\big)^{J-\mu} \psi_n \Big|^2, \end{aligned}$$

with $s^{\bar\alpha}_n = s^{1-\alpha}_n$ and $s^{\bar\beta}_n = s^{1-\beta}_n$. Introducing the conditional probability $P^\mu_\alpha(n) = \binom{J}{\mu}|s^\alpha_n|^{2\mu}|s^{\bar\alpha}_n|^{2(J-\mu)}$ for measuring μ of the J qubits in the state α after interaction with the system in state $|n\rangle$, we can separate the system and detector response in the above equation,

$$P^{\mu\nu}_{\alpha\beta} = \sum_{n,n',m} [U_{mn}\psi_n U^*_{mn'}\psi^*_{n'}] P^\mu_\alpha(n,n') P^\nu_\beta(m), \tag{34}$$

with the "off-diagonal" conditional probabilities $P^\mu_\alpha(n,n') = \binom{J}{\mu}(s^\alpha_n s^{\alpha\,*}_{n'})^\mu (s^{\bar\alpha}_n s^{\bar\alpha\,*}_{n'})^{(J-\mu)}$ [note that $P^\mu_\alpha(n,n) = P^\mu_\alpha(n)$]. The conditional probabilities $P^\mu_\alpha(n)$ depend only on the eigenvalue O_n of the state $|n\rangle$ (and not on the state $|n\rangle$ itself). We then have to distinguish two cases: (i) all system eigenvalues are nondegenerate, i.e., $O_n \neq O_{n'}$ for $n \neq n'$, and (ii) there are degenerate system states.

In the nondegenerate case (i) and for a strong measurement, the probability distributions $P^\mu_\alpha(n)$ and $P^\mu_\alpha(n')$ for different $n \neq n'$ do not overlap as functions of μ (this is the very definition of this measurement being a strong one), and the "off-diagonal" elements $P^\mu_\alpha(n,n')$ for $n' \neq n$ are suppressed, as follows from the relation $|P^\mu_\alpha(n,n')| = \sqrt{P^\mu_\alpha(n)P^\mu_\alpha(n')}$. We can then simplify expression (34) to the form $P^{\mu\nu}_{\alpha\beta} \approx \sum_{n,m} |U_{mn}\psi_n|^2 P^\mu_\alpha(n) P^\nu_\beta(m)$. The register correlators (replacing the distribution functions $P_{\alpha\beta}$) take the form

$$\begin{aligned} S_{\alpha\beta}(\tau_{21}) &= \langle\Psi_f| \sum_{j=1}^{J} \hat{p}^{(j)}_\alpha \sum_{j=J+1}^{2J} \hat{p}^{(j)}_\beta |\Psi_f\rangle = \sum_{\mu,\nu} \mu\nu P^{\mu\nu}_{\alpha\beta} \\ &= \sum_{n,m} |U_{mn}\psi_n|^2 \sum_\mu \mu P^\mu_\alpha(n) \sum_\nu \nu P^\nu_\beta(m). \end{aligned} \tag{35}$$

Assuming again a linear system-qubit coupling $\hat{H}_{\mathrm{sd}}(\tau) = \Omega(\tau)\hat{\sigma}_x\hat{O}$ that rotates the qubits by an angle $\delta\vartheta\ O_n$ around the x axis, the evolution

$$\hat{u}_n = \begin{pmatrix} \cos(\delta\vartheta\ O_n) & -i\sin(\delta\vartheta\ O_n) \\ i\sin(\delta\vartheta\ O_n) & \cos(\delta\vartheta\ O_n) \end{pmatrix} \tag{36}$$

produces the memory states $|\phi^{(j)}_n\rangle = \hat{u}_n|\phi^{(j)}_{\mathrm{in}}\rangle$, where we again assume initial states polarized in the xy plane; see (22). The probabilities $P_\alpha(n)$ for an individual qubit to reside in state $\alpha = 0,1$ are given by

$$P_0(n) = 1 - P_1(n) \approx \tfrac{1}{2} + (1-2\alpha)\delta\vartheta\ O_n \sin\theta. \tag{37}$$

With the qubits initially polarized along the y axis, i.e., $\theta^{(j)} = \pi/2$, we define the register's "magnetizations"

$$M(n) = \sum_\mu \mu\big[P^\mu_0(n) - P^\mu_1(n)\big] = 2J\delta\vartheta\ O_n, \tag{38}$$

where we have made use of (37) in the preceding equation. The combination $S_{11} - S_{10} - S_{01} + S_{00}$ then involves the product of register polarizations $M(n)M(m)$, and using the relation

$S^P_{OO}(\tau_{21}) = \sum_{nm} O_n O_m |U_{mn}\psi_n|^2$ [see Eq. (32)], we can relate the system correlator to the register correlators via

$$S^P_{OO}(\tau_{21}) = \frac{S_{11} - S_{10} - S_{01} + S_{00}}{4J^2\delta\vartheta^2}. \tag{39}$$

Note the normalization $S_{11} + S_{10} + S_{01} + S_{00} = J^2$, which follows from replacing $M(n) = \sum_\mu \mu[P^\mu_0(n) - P^\mu_1(n)]$ by $\Sigma(n) = \sum_\mu \mu[P^\mu_0(n) + P^\mu_1(n)] = \langle\mu\rangle_0 + \langle\mu\rangle_1 = J$.

In the degenerate case (ii), the distribution functions separate only for states with different eigenvalues $O_n \neq O_{n'}$, implying that $P^\mu_\alpha(n,n') \sim 0$, while for degenerate eigenvalues with $O_n = O_{n'}$, $P^\mu_\alpha(n,n') = P^\mu_\alpha(n)$. The probabilities $P^{\mu\nu}_{\alpha\beta}$ are then given by

$$P^{\mu\nu}_{\alpha\beta} \approx \sum_{m,n} \sum_{\{n'|O_{n'}=O_n\}} [U_{mn}\psi_n U^*_{mn'}\psi^*_{n'}] P^\mu_\alpha(n) P^\nu_\beta(m).$$

On the other hand, the projected density matrix $\rho^P(\tau_1)$ appearing in the system correlator $S^P_{OO}(\tau_{21})$ involves the projectors $\hat{P}_O = \sum_{\{n|O_n=O\}} |n\rangle\langle n|$, such that the result (39) remains unchanged.

Summarizing, we have seen that the measurement scheme invoking entanglement with quantum memories and their delayed measurement provides us, in the weak- and strong-measurement limits, with the same results as those obtained via the traditional route using an intermediate von Neumann projection. Furthermore, these results have been obtained within a unified description starting from the same initial formula in the form (5) or (6).

The above general theoretical considerations are rather nontrivial to implement in a practical situation, as the preparation, entanglement, and measurement of many quantum memories is often a nontrivial task. The implementation of these ideas is less demanding, though still challenging, when considering specific examples. Indeed, quantum memories for delayed measurement are naturally provided in a scattering geometry, where individual scattered particles take the role of flying qubits. In the following, we focus on a specific example in mesoscopic physics, i.e., the measurement of a charge correlator of a quantum dot by scattering electrons in a nearby quantum point contact. We first analyze the situation for a simple two-state system with charges $Q = ne$, $n = 0,1$, and then we extend these considerations to arbitrary charge states.

III. CHARGE-CORRELATOR MEASUREMENT

We consider a classic problem [21], namely the charge $\hat{Q}$ dynamics of a quantum dot (QD) (attached to leads or coupled to another dot in an isolated double-dot system) measured by a nearby quantum point contact (QPC); see Fig. 2 and Ref. [13] for a recent discussion of this system. Here, we want to characterize the dot's dynamics by its two-time charge correlator. In this system, the measurement is executed by the electrons that are transmitted across/reflected by the QPC with probabilities that depend on the dot's charge state. For the present discussion, it is convenient to view the QPC current as a sequence of individual electron pulses; during recent years, this theoretical idea [5,26,27] has progressed to an experimental reality [22–24], opening the new field of electron quantum optics [28]. The quantum memories can then be viewed as

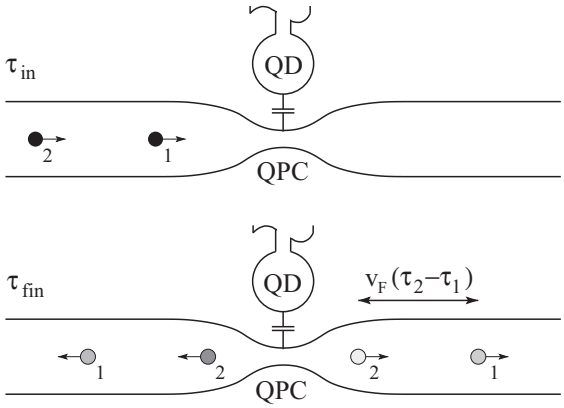

FIG. 2. Quantum dot system (QD) measured by a capacitively coupled quantum point contact (QPC): Single-electron pulses incident on the QPC from the left (at $\tau_{\rm in}$) are either transmitted (with amplitude t) or reflected (amplitude r); the outgoing Lippmann-Schwinger wave functions describe flying qubits without own dynamics, and they serve as quantum memories. Two pulses separated in time by $\tau_2 - \tau_1$ are needed to measure the two-time correlator of the dot's charge. After scattering at the QPC, the two electrons (flying qubits) are entangled with the quantum dot system and carry information on its dynamics. Simultaneous detection of the two scattered electrons (at $\tau_{\rm fin}$), e.g., a distance $v_F(\tau_2 - \tau_1)$ away with both positions on the right of the QPC, provides information on the two-time charge correlator.

flying qubits, individual electron pulses arriving at the QPC at times τ_1 and τ_2 that probe the charge state of the QD through the capacitive coupling between the QD and the QPC; see Fig. 2.

The memory states $|\varphi^{(j)}_\alpha\rangle$ are the two scattered states where the electron is reflected ($\alpha = {\rm r}$) or transmitted ($\alpha = {\rm t}$), i.e., the outgoing state is given by $|\phi^{(j)}_n\rangle = t_n|\varphi^{(j)}_{\rm t}\rangle + r_n|\varphi^{(j)}_{\rm r}\rangle$ with scattering coefficients $t_n \leftrightarrow s^{\rm t}_n$ and $r_n \leftrightarrow s^{\rm r}_n$ depending on the charge state of the system. We assume well-separated single-electron pulses and an evolution of the scattered waves $|\varphi^{(j)}_{\rm r,t}\rangle$ emanating from the QPC at times τ_j that preserves the corresponding system information, in particular $\langle\phi^{(2)}_m|\phi^{(1)}_n\rangle = 0$. This allows us to envision an individual detection of the electrons [24,29]. In the final readout, the flying qubits are detected on the right or left side of the QPC, telling whether the two electrons have been transmitted (with probability $P_{\rm tt}$), reflected ($P_{\rm rr}$), or mixed ($P_{\rm tr}$ and $P_{\rm rt}$). These probabilities then contain the information about the two-time charge correlator of the QD.

Formally, such a final-state analysis corresponds to measuring the (charge) operators $\hat{a}^{(j)} = \sum_\alpha a^{(j)}_\alpha \hat{p}^{(j)}_\alpha$, with the projectors $\hat{p}^{(j)}_\alpha = |\varphi^{(j)}_\alpha\rangle\langle\varphi^{(j)}_\alpha|$ providing the transmitted ($\alpha = {\rm t}$) or reflected ($\alpha = {\rm r}$) components of the jth electron. The eigenvalues $a^{(j)}_\alpha$ depend on the measured charge, e.g., $a^{(j)}_{\rm t} = 1$ and $a^{(j)}_{\rm r} = 0$ if the transmitted charge is measured on the right of the QPC, while $a^{(j)}_{\rm r} = 1$ and $a^{(j)}_{\rm t} = 0$ if the reflected charge is measured on the left. Both types of measurements provide us with the same probability distributions (5) or (6) with $\alpha,\beta = {\rm r,t}$.

In the following, we first analyze the case of a QD with binary charge states $|0\rangle$ and $|1\rangle$ and eigenvalues $Q_0 = 0$, $Q_1 = 1$, $\hat{Q} = |1\rangle\langle 1|$ (defined in units of e) and an initial state

$|\psi(\tau_{\rm in})\rangle = \psi_0(\tau_{\rm in})|0\rangle + \psi_1(\tau_{\rm in})|1\rangle$; see Eq. (1). Second, we generalize the discussion to a QD with multiple charge states as described by the charge operator $\hat{Q} = \sum_n Q_n|n\rangle\langle n|$. While two-state quantum memories (qubits) are always sufficient for a complete description when the measurement is weak, for a strong measurement a QD with multiple charge states will require the use of qubit registers, i.e., finite trains of electron pulses.

A. Weak measurement

For the case of a weak measurement, we can make immediate use of the general results Eqs. (17), (20), and (21) by replacing $\hat{O} \to \hat{Q}$ and choosing the values α,β equal to r and t. It remains to determine the detector response functions (19) and (18). We consider a linear system-detector coupling of the form $H_{\rm sd} = e^2\hat{q}\hat{Q}/C = \hat{v}\hat{Q}$, with $\hat{q}$ the charge on the QPC. Furthermore, we parametrize the scattering matrices for the system in states $|0\rangle$ and $|1\rangle$ by $t_0 = \sqrt{T}\,e^{i\theta}$, $r_0 = \sqrt{R}\,e^{i\chi}$, $t_1 = \sqrt{T-\delta T}\,e^{i(\theta+\delta\theta)}$, and $r_1 = \sqrt{R+\delta T}\,e^{i(\chi+\delta\chi)}$, with small corrections δT, $\delta\theta$, and $\delta\chi$.

To find the detector response functions (18) and (19), we replace $\hat{b}$ by $\hat{v}$ and determine the integral $(-i/\hbar)\int_{\tau_{\rm in}}^{\tau_f} d\tau\langle\phi_{\rm in}|\hat{p}_\alpha(j)(\tau_f)\hat{v}(\tau)|\phi_{\rm in}\rangle$ (we drop the memory index $^{(j)}$ as the electrons are scattered by the same QPC). To lowest order in $\hat{v}$, this can be written in the form $\langle\phi_{\rm in}|\hat{u}_0^\dagger\hat{p}_\alpha\hat{u}_1|\phi_{\rm in}\rangle - \langle\phi_{\rm in}|\hat{u}_0^\dagger\hat{p}_\alpha\hat{u}_0|\phi_{\rm in}\rangle$, with $\hat{u}_0 = e^{-i\hat{h}_0(\tau_f-\tau_{\rm in})/\hbar}$ and $\hat{u}_1 = e^{-i(\hat{h}_0+\hat{v})(\tau_f-\tau_{\rm in})/\hbar}$ describing the dynamics of the detector in the Heisenberg representation in the absence and presence of a charge on the dot, respectively. Furthermore, we have used that $\hat{u}_1 = \hat{u}_0\hat{u}_D$ with

$$\hat{u}_D = \mathcal{T}\exp\left(-i\int_{\tau_{\rm in}}^{\tau_f} d\tau\,\hat{v}(\tau)/\hbar\right) \tag{40}$$

and $\hat{v}(\tau)$ in the interaction representation. The initial memory states $|\phi_{\rm in}\rangle$ evolve under $\hat{u}_1$ and $\hat{u}_0$ according to $\hat{u}_n|\phi_{\rm in}\rangle = |\phi_n\rangle$ and hence $\langle\phi_{\rm in}|\hat{u}_m^\dagger\hat{p}_\alpha\hat{u}_n|\phi_{\rm in}\rangle = \langle\phi_m|\hat{p}_\alpha|\phi_n\rangle = s_m^{\alpha*}s_n^\alpha$, where we have used that $\hat{p}_\alpha = |\varphi_\alpha\rangle\langle\varphi_\alpha|$. Expanding s_1^α in δT, $\delta\theta$, and $\delta\chi$, we find that

$$\frac{-i}{\hbar}\int_{\tau_{\rm in}}^{\tau_f} d\tau\langle\phi_{\rm in}|\hat{p}_{\rm t}(\tau_f)\hat{v}(\tau)|\phi_{\rm in}\rangle = -\frac{1}{2}\delta T + iT\delta\theta, \tag{41}$$

$$\frac{-i}{\hbar}\int_{\tau_{\rm in}}^{\tau_f} d\tau\langle\phi_{\rm in}|\hat{p}_{\rm r}(\tau_f)\hat{v}(\tau)|\phi_{\rm in}\rangle = \frac{1}{2}\delta T + iR\delta\chi, \tag{42}$$

and taking real and imaginary parts, we arrive at the final results,

$$\mathcal{R}S_{\rm det,t} = T\delta\theta, \quad \mathcal{R}S_{\rm det,r} = R\delta\chi, \tag{43}$$

$$\mathcal{I}S_{\rm det,t} = -\delta T, \quad \mathcal{I}S_{\rm det,r} = \delta T. \tag{44}$$

Using these detector response functions in the general expressions (20) and (21), one easily arrives at the system correlators (we choose $\alpha = {\rm t}$, $\bar{\alpha} = {\rm r}$, and $\beta = {\rm t}$),

$$\mathcal{R}S_{QQ}^{\rm irr} = \frac{R(\delta\chi/\delta T)\,P_{\rm tt}^{\rm irr} - T(\delta\theta/\delta T)\,P_{\rm rt}^{\rm irr}}{\delta T\,(R\delta\chi + T\delta\theta)}, \tag{45}$$

$$\mathcal{I}S_{QQ}^{\rm irr} = -\frac{P_{\rm tt}^{\rm irr} + P_{\rm rt}^{\rm irr}}{\delta T\,(R\delta\chi + T\delta\theta)}. \tag{46}$$

Alternatively, the QPC can be tuned to deliver the individual system correlators $\mathcal{R}S_{QQ}^{\rm irr}$ or $\mathcal{I}S_{QQ}^{\rm irr}$. Indeed, using a detector with high transmission, e.g., a QPC with energetic (E) single-electron pulses $E \gg V_0$, where V_0 is the QPC barrier, one easily finds that (although $\delta T \ll |\delta\theta|, |\delta\chi|$, we have $\delta T \gg R|\delta\chi|$)

$$|\mathcal{R}S_{\rm det,t}| \gg |\mathcal{I}S_{\rm det,r/t}| \gg |\mathcal{R}S_{\rm det,r}|, \tag{47}$$

and therefore $P_{{\rm t}\beta}^{\rm irr}$ measures $\mathcal{I}S_{QQ}^{\rm irr}$, while $P_{{\rm r}\beta}^{\rm irr}$ measures $\mathcal{R}S_{QQ}^{\rm irr}$. When the detector predominantly reflects particles, e.g., for low-energy single-electron pulses with $E \ll V_0$, the situation is reverse, $|\mathcal{R}S_{\rm det,r}| \gg |\mathcal{I}S_{\rm det,r/t}| \gg |\mathcal{R}S_{\rm det,t}|$, and $\mathcal{I}S_{QQ}^{\rm irr}$ ($\mathcal{R}S_{QQ}^{\rm irr}$) is measured by $P_{{\rm r}\beta}^{\rm irr}$ ($P_{{\rm t}\beta}^{\rm irr}$); see the Appendix for further details on the QPC detector response.

For a quantum dot with multiple charge states, we have to require that the expansion of the scattering amplitudes $t_n = \sqrt{T_n}e^{i\theta_n}$ and $r_n = \sqrt{1-T_n}e^{i\chi_n}$ of the QPC detector scale linearly in the charge Q_n of the dot, i.e., $T_n = T - Q_n\delta T$, $\theta_n = \theta + Q_n\delta\theta$, and $\chi_n = \chi + Q_n\delta\chi$. A straightforward calculation then shows that the results (43) and (44) for the detector response functions as well as the final results (45) and (46) remain unchanged.

B. Strong measurement

When performing a strong measurement of a quantum dot with a binary charge, it is sufficient to invoke individual electron pulses as quantum memories. For a strong dot–QPC coupling, we require a one-to-one relation between the presence of a charge on the dot and the outcome of the measurement, i.e., $|\phi_0\rangle = |\varphi_{\rm t}\rangle$ and $|\phi_1\rangle = |\varphi_{\rm r}\rangle$ [see Eq. (29)] or $s_1^{\rm r} = 1$ and $s_0^{\rm r} = 0$. This is achieved by tuning the QPC so as to generate a unique scattering outcome with $|r_1| = 1$, $|r_0| = 0$ and $|t_0| = 1$, $|t_1| = 0$, i.e., the presence of a charge $Q_1 = 1$ on the dot reflects the QPC electron back to the left. In this case, it is the reflection probability $P_{\rm rr}(\tau_{21})$ that directly traces the charge $\hat{Q}$, and according to (6) we have to evaluate the expression

$$P_{\rm rr}(\tau_{21}) = \sum_m \left|\sum_n r_m U_{mn}(\tau_{21}) r_n \psi_n(\tau_1)\right|^2. \tag{48}$$

With $r_m = \delta_{m1}$, we obtain the simple result $P_{\rm rr}(\tau_{21}) = |U_{11}(\tau_{21})\psi_1|^2$ [see also (30) with $n,m = 1$ and $\alpha_1 = \beta_1 = {\rm r}$], and since $Q_n = \delta_{n1}$, we find the projected correlator [see Eq. (32)]

$$S_{QQ}^P(\tau_1,\tau_2) = P_{\rm rr}(\tau_{21}) = |U_{11}(\tau_{21})\psi_1|^2. \tag{49}$$

Similarly, the probability to find no charge on the dot in either of the two measurements is $P_{\rm tt} = |U_{00}\psi_0|^2$, while the mixed results are $P_{\rm tr} = |U_{10}\psi_0|^2$ and $P_{\rm rt} = |U_{01}\psi_1|^2$.

The strong measurement of the charge correlator for a multicharge quantum dot quite naturally involves trains of electron pulses [19], with the number J of electrons in each train sufficiently large to distinguish the different charge eigenvalues Q_n of the dot. The separation $\delta\tau$ between electron pulses within a train has to be sufficiently long in order to allow for their separate detection (i.e., counting), while the train duration $J\,\delta\tau$ must remain small on the scale $\tau_{\rm sys}$ of the dot's dynamics.

When going over from qubit registers to electron trains scattered at the QPC, we replace the "magnetization" (38) by the imbalance between reflected and transmitted electrons,

$$D(n) = \sum_{\mu} \mu\big[P_{\rm r}^{\mu}(n) - P_{\rm t}^{\mu}(n)\big] = J[R - T + 2Q_n\delta R], \tag{50}$$

where we have assumed a linear QPC characteristic with a reflection probability scaling linearly with the dot's charge Q_n, $R_n = R + Q_n\delta R$. Operating the QPC at the symmetry point $T = R = 1/2$, we can determine the combination $S_{\rm rr} - S_{\rm rt} - S_{\rm tr} + S_{\rm tt}$ and relate this quantity to the projected charge correlator $S^P_{QQ}(\tau_{21})$,

$$S^P_{QQ}(\tau_{21}) = \frac{S_{\rm rr} - S_{\rm rt} - S_{\rm tr} + S_{\rm tt}}{4J^2\delta R^2}. \tag{51}$$

Operating the QPC away from the symmetric point, one has to determine the weighted sum $T^2 S_{\rm rr} - TR\, S_{\rm rt} - RT\, S_{\rm tr} + R^2 S_{\rm tt}$ instead and divide by $J^2\delta R^2$ to arrive at the projected correlator S^P_{QQ}.

C. Finite-width memory wave packets

Above, we have assumed an instantaneous (within a short time $\delta\tau$) entanglement between the system and the memory states, requiring that both the width $\tau_{\rm wp}$ of the wave packet and the scattering time $\tau_{\rm sca}$ at the QPC satisfy $\tau_{\rm wp}, \tau_{\rm sca} \ll \tau_{\rm sys}$, where $\tau_{\rm sys}$ denotes the characteristic time scale of the system. Here, we allow for a spread in time of the detector's electron wave function, and we drop the condition $\tau_{\rm wp} \ll \tau_{\rm sys}$, i.e., we assume that $\tau_{\rm wp} \lesssim \tau_{\rm sys}$ while the scattering event itself remains fast, $\tau_{\rm sca} \ll \tau_{\rm sys}$. In general terms, this corresponds to a measurement that probes the system sharply ($\tau_{\rm sca} \ll \tau_{\rm sys}$) during some finite time ($\tau_{\rm wp} \lesssim \tau_{\rm sys}$; longer measurement times $\tau_{\rm wp} > \tau_{\rm sys}$ do not provide meaningful results).

Let us suppose that the jth wave packet incident on the QPC around τ_j is described by the wave function $f^{(j)}(\tau)$, which is normalized [$\int d\tau |f^{(j)}(\tau)|^2 = 1$] and peaked at the time τ_j. Assuming instantaneous scattering, we obtain the final state

$$|\tilde\Psi_f\rangle = \int d\tau_1'\, f^{(1)}(\tau_1') \int d\tau_2'\, f^{(2)}(\tau_2') \times \sum_{l,m,n} U_{lm}(\tau_{f2}')U_{mn}(\tau_{21}')\psi_n(\tau_1')\,|l\rangle\,\big|\phi_n^{(1)}(\tau_1')\big\rangle\,\big|\phi_m^{(2)}(\tau_2')\big\rangle, \tag{52}$$

with $\tau_{f2}' = \tau_f - \tau_2'$ and $\tau_{21}' = \tau_2' - \tau_1'$ and the outgoing memory states $|\phi_n^{(j)}(\tau_j')\rangle$ that have been scattered at the QPC at time τ_j'. Making use of $\langle\phi_{n'}^{(j)}(\tau_j'')|\phi_n^{(j)}(\tau_j')\rangle = \delta(\tau_j' - \tau_j'')\langle\phi_{n'}^{(j)}|\phi_n^{(j)}\rangle$, we obtain the smeared probabilities

$$\tilde P_{\alpha\beta}(\tau_{21}) = \int d\tau_1' \int d\tau_2'\, |f^{(1)}(\tau_1')|^2 |f^{(2)}(\tau_2')|^2 P_{\alpha\beta}(\tau_{21}') \tag{53}$$

with $P_{\alpha\beta}$ given by Eq. (6). The finite-width wave packets enter as integration kernels. While for sharp wave packets the entanglement between system and memories (i.e., the "measurement") takes place at times τ_1 and τ_2, for broader wave packets the entanglement arises within a finite time $\tau_{\rm wp}$ around τ_1 and τ_2 with distribution functions $|f^{(1)}(\tau_1')|^2$ and $|f^{(2)}(\tau_2')|^2$. As a consequence, for the case of strong coupling where the entanglement gives rise to projective measurements, the times of projection are not fixed but are distributed with the distribution functions above.

Note that the result (53) is only valid for negligible scattering time $\tau_{\rm sca}$ in the QPC. If the scattering time $\tau_{\rm sca}$ is finite compared to the system time $\tau_{\rm sys}$, the effect of interaction cannot be accounted for by the scattering matrices $\hat s_n$ of the QPC depending on the system state, but the interaction during the scattering has to be treated in more detail.

The limit of $\tau_{\rm sca} \ll \tau_{\rm sys}$ considered above also has implications for the resulting backaction: While the backaction for $\tau_{\rm sca} \ll \tau_{\rm sys}$ only consists of dephasing, i.e., a suppression of off-diagonal elements of the system's density matrix, for finite $\tau_{\rm sca}$ the backaction of the measurement on the system goes beyond pure dephasing and alters the system's dynamics.

D. Higher-order correlators

The study of higher-order correlators is straightforward, e.g., to measure a third-order charge correlator we send three electrons scattering from the QPC at times $\tau_1 < \tau_2 < \tau_3$ and obtain the probabilities

$$P_{\alpha\beta\gamma} = \sum_l \left| \sum_{m,n} s_l^{\gamma} U_{lm}(\tau_{32}) s_m^{\beta} U_{mn}(\tau_{21}) s_n^{\alpha} \psi_n(\tau_1) \right|^2 \tag{54}$$

describing electrons transmitted across ($\alpha,\beta,\gamma = {\rm t}$) or reflected from ($\alpha,\beta,\gamma = {\rm r}$) the QPC. For weak coupling, its irreducible part can be recast in the form

$$P^{\rm irr}_{\alpha\beta\gamma} = \sum_{\sigma\sigma'=\pm} S^{(1),\bar\sigma}_{{\rm det},\alpha} S^{(2),\bar\sigma'}_{{\rm det},\beta} S^{(3),-}_{{\rm det},\gamma}\, S^{\sigma\sigma',{\rm irr}}_{QQQ}(\tau_1,\tau_2,\tau_3) \tag{55}$$

with $\bar\sigma = -\sigma$, the detector responses $S^{(j),+}_{{\rm det},\alpha} = \mathcal{R} S^{(j)}_{{\rm det},\alpha}$ and $S^{(j),-}_{{\rm det},\alpha} = \mathcal{I} S^{(j)}_{{\rm det},\alpha}$, and the third-order correlators

$$S^{\sigma\sigma',{\rm irr}}_{QQQ} = c_\sigma c_{\sigma'} \langle\!\langle [\hat Q(\tau_1), [\hat Q(\tau_2), \hat Q(\tau_3)]_{\sigma'}]_\sigma \rangle\!\rangle \tag{56}$$

with the constants $c_+ = 1/2$ and $c_- = -i$, and $[\cdot,\cdot]_- = [\cdot,\cdot]$ and $[\cdot,\cdot]_+ = \{\cdot,\cdot\}$, respectively [note that (anti)symmetrized charges in $S^{\rm irr}_{QQQ}$ (encoded in σ) relate to opposite detector response functions (encoded by $\bar\sigma$)]. This result agrees with the one in Ref. [4] obtained with the help of the von Neumann projection postulate, and it shows that only *Keldysh time-ordered charge correlators* are measurable.

E. Experimental implementation

Our general concept of deferred repeated measurements has been formulated with quantum memories, e.g., qubits, qubit registers, and qudits; see Sec. II. In our application of these general considerations, the measurement of a charge correlator with the help of a quantum point contact (Sec. III), the quantum memories have been replaced by scattered electrons (flying qubits). It is then natural to seek an experimental implementation, where the final measurement of the quantum memories, i.e., the scattered electrons, can be cast into a measurement of currents and noise rather than an individual detection of qubit states. Such an implementation is proposed below.

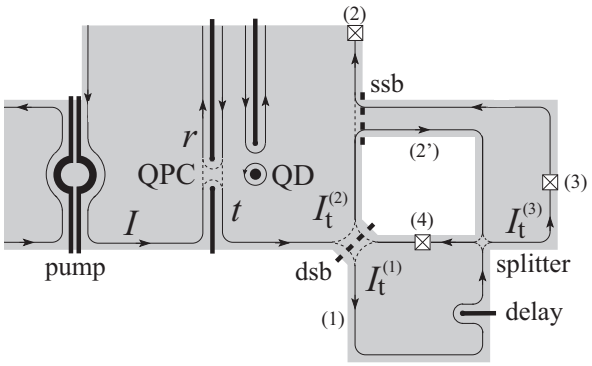

FIG. 3. Schematic illustration of a quantum Hall device with a single-electron pump (left), the QPC-QD setup (middle), and a detector arrangement (right), inspired by Refs. [23,24]. Pairs of electrons are injected by the single-electron pump with a time delay τ_{21} and scattered by the quantum point contact with scattering coefficients r and t depending on the charge state of the quantum dot. The dynamically switchable barrier [23] (dsb) separates the first and second electron (flying qubits $j = 1$ and 2) into arms 1 and 2. Closing the static switchable barrier (ssb) and measuring the currents $I_t^{(1)} = I_t^{(3)} + I_t^{(4)}$ and $I_t^{(2)}$ provides the antisymmetrized charge-charge correlator $\mathcal{I}S_{QQ}^{\rm irr}$. Opening the static switchable barrier (ssb), having the two-particle streams along the trajectories 1 and 2′ interfere at the 50/50 beam splitter, and measuring the current noise $S^{(3)}(\tau)$ as a function of the tunable delay τ in detector 3 provides the symmetrized correlator $\mathcal{R}S_{QQ}^{\rm irr}$.

By now, several experiments have demonstrated the controlled generation of individual electron pulses [22–24], and even the detection of such pulses via qubit detectors seems to be in reach [29]. A setup particularly well suited within the current context is that of Fletcher *et al.* [23], involving a single-electron pump and a time-correlated detector setup in a quantum Hall device; see Fig. 3 for an illustration. Pairs of electron pulses of width ∼100 ps are injected at a typical rate $\nu_p \sim (10\ \text{ns})^{-1}$ and are well suited to probe the dynamics of a dot with a system time $\tau_{\rm sys} \sim$ 100–1000 ns. The detector involves a dynamically switchable barrier (dsb in Fig. 3) that can be switched on or off with a nanosecond precision in time.

We propose an experiment implementing a weak measurement of a charge correlator along the lines of Sec. III A, where electron pairs with a tunable delay time in the range $\tau_{21} = 10$–100 ns are injected by the single-electron pump (with injection currents in the $I = 2e\nu_p \sim 10$ pA regime) and scattered at the QPC probing the quantum dot QD. The transmitted electrons arrive at the detector dsb after a delay time τ_d. The detector barrier dsb is switched on at a time $\tau_d + \tau_{21}/2$ in order to let the first electron pass along the path 1 and deflect the second electron along 2; see Fig. 3. With the static barrier (ssb) closed, the measured currents $I_t^{(1)}$ and $I_t^{(2)}$ resulting from the transmission of the first and second electron, respectively, can be related to the probabilities $P_{\alpha\beta}$ via

$$I_t^{(1)}/e\nu_p = P_{\rm tt} + P_{\rm tr}, \tag{57}$$

$$I_t^{(2)}/e\nu_p = P_{\rm tt} + P_{\rm rt}. \tag{58}$$

The two sums $\sum_\beta P_{\alpha\beta}$ and $\sum_\alpha P_{\alpha\beta}$ in the above equations are fundamentally different in a subtle way: summing over the second particle β produces the trivial probability $P_\alpha^{(1)} = \langle\Psi_f|\hat{p}_\alpha^{(1)}|\Psi_f\rangle$ for the (independent) transmission ($\alpha = $ t) or reflection ($\alpha = $ r) of the first electron by the QPC, $\sum_\beta P_{\alpha\beta} = P_\alpha^{(1)}$. Hence, the first equation (57) reduces to $I_t^{(1)}/e\nu_p = P_t^{(1)}$ and thus contains only information about the mean charge on the dot.

On the contrary, summing over the first particle α *does not* generate $P_\beta^{(2)}$ as the interaction of the first electron at the earlier time τ_1 introduces nontrivial correlations, see Eq. (6). This becomes apparent when going over to irreducible probabilities $P_{\alpha\beta}^{\rm irr} = P_{\alpha\beta} - P_\alpha^{(1)}P_\beta^{(2)}$ and using the normalization $\sum_\alpha P_\alpha^{(j)} = 1$. Then, the second equation (58) becomes $I_t^{(2)}/e\nu_p = P_{\rm tt}^{\rm irr} + P_{\rm rt}^{\rm irr} + P_t^{(2)}$ which includes information about the dot's charge correlator. Assuming a time-independent mean charge on the dot, we have $P_t^{(2)} = P_t^{(1)} = I_t^{(1)}/e\nu_p$ and using the general result (17), the measured currents are easily transformed to provide the antisymmetrized correlator

$$\mathcal{I}S_{QQ}^{\rm irr} = \frac{\left(I_t^{(2)} - I_t^{(1)}\right)/e\nu_p}{\delta T(R\delta\chi + T\delta\theta)}. \tag{59}$$

Note that the evaluation of the irreducible probability $P_{\rm tt}^{\rm irr} + P_{\rm tr}^{\rm irr}$ with the help of (17) indeed provides a vanishing result, $P_{\rm tt}^{\rm irr} + P_{\rm tr}^{\rm irr} \propto (\mathcal{I}S_{\rm det,r} + \mathcal{I}S_{\rm det,t}) = 0$, explicitly demonstrating that the sum $P_{\rm tt}^{\rm irr} + P_{\rm tr}^{\rm irr}$ contains no correlations.

To find the symmetric correlator $\mathcal{R}S_{QQ}^{\rm irr}$, one has to measure a time correlator on the transmitted channel. This can be conveniently done with the help of a Hong-Ou-Mandel-type splitter as implemented in the experiment of Bocquillon *et al.* [24] and sketched in Fig. 3. In this experiment, the dynamically switchable barrier (dsb) again splits the two electrons in each pair to propagate along the paths 1 and $2 \to 2'$, respectively. The static barrier (ssb) is left open, such that the two particles interfere in the splitter. Measuring the current noise $S^{(3)}(\tau)$ in channel 3 as a function of mutual delay τ (tuned via an additional gate in loop 1; see the figure) then provides all information needed to construct $\mathcal{R}S_{QQ}^{\rm irr}$.

We can calculate the evolution of the state through the Hong-Ou-Mandel setup using the wave function $|\Psi_f\rangle = |\Psi_f\rangle_{\rm tt} + |\Psi_f\rangle_{\rm tr} + |\Psi_f\rangle_{\rm rt} + |\Psi_f\rangle_{\rm rr}$ describing the two-electron state after the scattering events at the QPC, with $P_{\alpha\beta} = {}_{\alpha\beta}\langle\Psi_f|\Psi_f\rangle_{\alpha\beta}$, i.e., the individual components are not normalized and only $\langle\Psi_f|\Psi_f\rangle = 1$. Due to the orthogonality of these four components, the particle numbers $\hat{N}^{(i)}$, $i = 3,4$, emerging from our Hong-Ou-Mandel splitter can be analyzed term by term. In particular, the particle number fluctuations $\langle\Psi_f|(\delta\hat{N}_3)^2|\Psi_f\rangle$ in channel 3 involve single-particle and two-particle contributions, ${}_{\rm rt}\langle\Psi_f|\hat{N}_3|\Psi_f\rangle_{\rm rt} = (1/2)\times 1\times P_{\rm rt}$ and ${}_{\rm rt}\langle\Psi_f|\hat{N}_3^2|\Psi_f\rangle_{\rm rt} = (1/2)\times 1^2\times P_{\rm rt}$, hence

$${}_{\rm rt}\langle\Psi_f|(\delta\hat{N}_3)^2|\Psi_f\rangle_{\rm rt} = \tfrac{1}{4}P_{\rm rt}, \tag{60}$$

and the same result holds true for the $|\Psi_f\rangle_{\rm tr}$ scattering component. While there is no contribution from $|\Psi_f\rangle_{\rm rr}$, the one originating from $|\Psi_f\rangle_{\rm tt}$ depends on the time delay τ. Let $f_1(x)$ and $f_2(x)$ denote the two-electron wave packets propagating along the incoming paths 1 and 2 of the HOM interferometer. As shown in Ref. [30], we can relate the number fluctuation in

the component $|\Psi_f\rangle_{\rm tt}$ to the overlap of wave functions as

$$ {}_{\rm tt}\langle\Psi_f|(\delta\hat{N}_3)^2|\Psi_f\rangle_{\rm tt} = \tfrac{1}{2}(1-|\langle f_1|f_2\rangle|^2)P_{\rm tt}, \tag{61}$$

where $\langle f_1|f_2\rangle = \int dx f_1^*(x) f_2(x)$. For a large time delay between the first and second electron, these do not interfere, $\langle f_1|f_2\rangle = 0$, such that the fluctuations are just the double of (60),

$$ {}_{\rm tt}\langle\Psi_f|(\delta\hat{N}_3)^2|\Psi_f\rangle_{\rm tt} = \tfrac{1}{2}\,P_{\rm tt}. \tag{62}$$

Compensating the original time delay $\tau = -\tau_{21}$ (such that the two electrons arrive simultaneously at the splitter), we have

$$ {}_{\rm tt}\langle\Psi_f|(\delta\hat{N}_3)^2|\Psi_f\rangle_{\rm tt} = 0, \tag{63}$$

since the Pauli exclusion forces the two particles to propagate to different channels. The final result $\langle\Psi_f|(\delta\hat{N}_3)^2|\Psi_f\rangle$ then involves separately the probabilities $P_{\rm rt}+P_{\rm tr}$ and $P_{\rm tt}$,

$$ \langle\Psi_f|(\delta\hat{N}_3)^2|\Psi_f\rangle_\infty = \tfrac{1}{4}(P_{\rm rt}+P_{\rm tr})+\tfrac{1}{2}P_{\rm tt}, \tag{64}$$

when the delay between electron pulses is not compensated, and

$$ \langle\Psi_f|(\delta\hat{N}_3)^2|\Psi_f\rangle_0 = \tfrac{1}{4}(P_{\rm rt}+P_{\rm tr}), \tag{65}$$

when the time delay is properly compensated, $\tau = -\tau_{21}$.

In a next step, we express the charge fluctuations in channel 3 through the irreducible current-current correlator [30],

$$ \langle\Psi_f|(\delta\hat{N}_3)^2|\Psi_f\rangle = \frac{1}{e^2}\int_W dt_1 dt_2\, \langle\!\langle \hat{I}^{(3)}(t_1)\hat{I}^{(3)}(t_2)\rangle\!\rangle, \tag{66}$$

where the time window W is centered around the arrival time of the wave packets at the detector 3 and has a width of the order of $\Delta\tau = \nu_p^{-1}$, with ν_p the rate of pair injection by the pump. The particle number fluctuations then can be expressed through the low-frequency current noise $S^{(3)}(\omega)$,

$$ \langle\Psi_f|(\delta\hat{N}_3)^2|\Psi_f\rangle = \int \frac{d\omega}{2\pi}\,\frac{S^{(3)}(\omega)}{e^2}\,\frac{\sin^2(\omega/2\nu_p)}{(\omega/2)^2}, \tag{67}$$

with $\omega \leqslant \nu_p$. Neglecting the frequency dependence of the noise at small ω, $S^{(3)}(\omega) \sim S^{(3)}(0)$, we obtain

$$ \langle\Psi_f|(\delta\hat{N}_3)^2|\Psi_f\rangle = S^{(3)}/e^2\nu_p, \tag{68}$$

and hence

$$ P_{\rm rt}+P_{\rm tr} = 4\frac{S_0^{(3)}}{e^2\nu_p}, \quad P_{\rm tt} = 2\frac{S_\infty^{(3)}-S_0^{(3)}}{e^2\nu_p}. \tag{69}$$

Using Eq. (17), we can derive an alternative (more symmetrized) version of Eq. (45) that involves just the combinations $P_{\rm rt}^{\rm irr}+P_{\rm tr}^{\rm irr}$ and $P_{\rm tt}^{\rm irr}$,

$$ \mathcal{R}S_{QQ}^{\rm irr} = \frac{(R\delta\chi)^2\,P_{\rm tt}^{\rm irr} - T\delta\theta\,R\delta\chi\left(P_{\rm rt}^{\rm irr}+P_{\rm tr}^{\rm irr}\right)+(T\delta\theta)^2\,P_{\rm rr}^{\rm irr}}{(\delta T)^2(R\delta\chi+T\delta\theta)^2}. \tag{70}$$

Defining the detector parameters $\kappa = T\delta\theta/(R\delta\chi+T\delta\theta)$ and going over to irreducible probabilities (with $P_{\rm t}^{(1)} = P_{\rm t}^{(2)} = I_t^{(1)}/e\nu_p$ independent of time), we obtain the final result

$$ (\delta T)^2\,\mathcal{R}S_{QQ}^{\rm irr} = 2(1-2\kappa)\frac{S_\infty^{(3)}-S_0^{(3)}}{e^2\nu_p}+4\kappa\frac{S_0^{(3)}}{e^2\nu_p}+\kappa^2-\left(\frac{I_t^{(1)}}{e\nu_p}-\kappa\right)^2. \tag{71}$$

Note that in this setup, the final measurement of qubit memories does not require fast or time resolved detection schemes, but merely relies on the measurement of average currents and low-frequency noise. This is due to the fact, that all timing tasks are realized by the properly time-delayed electron pulses in the incoming channel and the dynamically switchable gate (dsb) which separates the electron pairs; both elements have been realized in an experiment [23]. Hence, the new measurement scheme, combined with novel elements from electron quantum optics, allows to shift the (difficult) timing issues in the measurement of a time-correlator from the detector to the source.

A *strong coupling* between the quantum dot and the quantum point contact provides us with a projected correlator. For the simplest case of a binary charge on the dot with values $Q = 0,1$, the projected charge correlator is given by Eq. (49), $S_{QQ}^P = P_{\rm rr}$. Making use of the normalization $P_{\rm tt}+P_{\rm rt}+P_{\rm tr}+P_{\rm rr} = 1$ and the result Eq. (69), we find that

$$ S_{QQ}^P = 1-2\,\frac{S_0^{(3)}+S_\infty^{(3)}}{e^2\nu_p}. \tag{72}$$

IV. CONCLUSION

In conclusion, we have applied the principle of deferred measurement to the problem of repeated measurement, and we have derived physical expressions for the two- and multitime correlators. The measurement involves the inclusion of quantum memories that are entangled with the system at specific times τ_j where the system observable is to be probed. The expanded system plus memories undergoes a unitary evolution until the very end, where the result is extracted via application of Born's rule to the memories. The measured probabilities $P_{\alpha\beta}$ [see Eq. (6)] or memory correlators $S_{\alpha\beta}$ [see Eq. (35)] can then be combined to extract the desired system correlators. The limits of weak and strong measurements provide the standard (anti)symmetrized and projected time correlators previously obtained by invoking the (nonunitary) von Neumann projection. The general results have been illustrated by using qubits and qubit registers as quantum memories. Our analysis sheds new light on the problem of repeated measurement, and it illustrates the usefulness of qubits as sensitive measurement devices.

Although our paper's main results are rather on the conceptual side, one could imagine an implementation of such a deferred measurement in an experiment. A system that naturally lends itself for a realization of these ideas is the classic mesoscopic setup, which probes the charge of a quantum dot through a quantum point contact. The individual scattered electrons in the QPC can be understood as flying qubits that are either transmitted or reflected, with amplitudes depending on the charge state of the quantum dot. In particular, the qubit register required in the strong measurement of a dot with a multivalued charge is easily implemented in terms of finite trains of electrons. We have applied our formalism to this situation and derived the corresponding expressions for a weak and strong measurement.

The experimental implementation of these ideas requires a system control that can only be met with a modern quantum engineering approach. Recent developments in electron quantum

optics provide controlled single-electron pulses and allow for their time-resolved manipulation/detection on a subnanosecond time scale [23,24]. Using the setup of Ref. [23] as a base and augmenting it with a Hong-Ou-Mandel-type analyzer [24], we propose to include a quantum point contact and a quantum dot in order to realize the principle of repeated measurement by a deferred measurement of quantum memories.

As a final remark, one may appreciate the relation of the deferred measurement principle to Everett's idea of a multiverse [31,32]. Rather than applying a projection after the first measurement and pursuing a single further evolution (of the system = "universe"), the principle of a deferred measurement involving the system's entanglement with a quantum memory enhances the overall dimensionality, e.g., for a qubit memory the dimensionality is doubled (with two "universes" evolving in parallel). It is then only the final measurement that determines which evolution (i.e., which "universe") has actually been realized.

ACKNOWLEDGMENTS

We thank Renato Renner for discussions and acknowledge financial support from the Swiss National Science Foundation through the National Center of Competence in Research on Quantum Science and Technology (QSIT), the Pauli Center for Theoretical Studies at ETH Zurich, and RFBR Grant No. 14-02-01287.

APPENDIX: DETECTOR PROPERTIES

A quick overview is provided by the example of a *δ-function scatterer:* Expressing the strength of the scatterer $\hbar^2\lambda/m$ for the two charge states by $\lambda_0 = \lambda$ and $\lambda_1 = \lambda + \delta\lambda$, an incoming state with wave vector k is transmitted with amplitude $t_n = k/(k + i\lambda_n)$, $n \in \{0,1\}$. Expanding the transmission $T_n = k^2/(k^2 + \lambda_n^2)$ and phase $\theta_n = -\arctan(\lambda_n/k)$, we find the modifications δT and $\delta\theta = \delta\chi$ (for a symmetric scatterer) in the scattering characteristic of the QPC upon charging the dot,

$$\delta T \approx -\frac{2k^2\lambda^2}{(k^2+\lambda^2)^2}\frac{\delta\lambda}{\lambda}, \tag{A1}$$

$$\delta\theta = \delta\chi = -\frac{k\lambda}{k^2+\lambda^2}\frac{\delta\lambda}{\lambda}. \tag{A2}$$

In the limit of a large incoming energy, i.e., $k \gg \lambda$, we find $\delta T \approx -2\lambda\,\delta\lambda/k^2$ and $\delta\theta = \delta\chi \approx -\delta\lambda/k$ and hence $\delta\theta, \delta\chi \gg \delta T$; with $T \approx 1$ and $R \approx \lambda^2/k^2 \ll 1$, we have $T|\delta\theta| \gg |\delta T| \gg R|\delta\chi|$ and therefore $|\mathcal{I}S_{\mathrm{det,t}}| \gg |\mathcal{R}S_{\mathrm{det,r/t}}| \gg |\mathcal{I}S_{\mathrm{det,r}}|$. For a small incoming energy $k \ll \lambda$, we obtain $\delta T \approx -2k^2\delta\lambda/\lambda^3$ and $\delta\theta \approx -k\delta\lambda/\lambda^2$, and using $T \approx k^2/\lambda^2$ and $R \approx 1$, we find $|\mathcal{I}S_{\mathrm{det,r}}| \gg |\mathcal{R}S_{\mathrm{det,r/t}}| \gg |\mathcal{I}S_{\mathrm{det,t}}|$. When $k \approx \lambda$, all response functions are of the same order.

Alternatively, we can consider a single electron transistor (SET) with the level position $k_{\mathrm{res},n}$ affected by the capacitive coupling and depending on the dot's charge state $|n\rangle$, i.e., $k_{\mathrm{res},0} = k_{\mathrm{res}}$ and $k_{\mathrm{res},1} = k_{\mathrm{res}} + \delta k_{\mathrm{res}}$. The transmission coefficient is given by $t_n = i\gamma/(k - k_{\mathrm{res},n} + i\gamma)$, where γ is the level width. Again expanding $T_n = \gamma^2/[(k - k_{\mathrm{res},n})^2 + \gamma^2]$ and $\tan\theta_n = (k - k_{\mathrm{res},n})/\gamma$ for small $\delta k_{\mathrm{res}} \ll k_{\mathrm{res}}$, we find

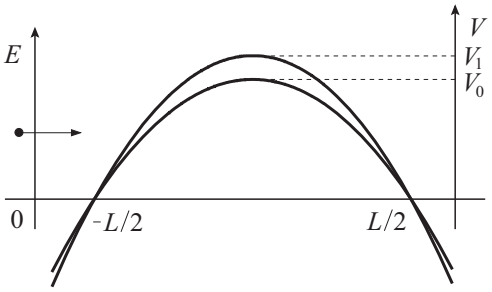

FIG. 4. QPC modeled by a parabolic potential.

$$\delta T = -\frac{2(k - k_{\mathrm{res}})\gamma^2\delta k_{\mathrm{res}}}{[(k - k_{\mathrm{res}})^2 + \gamma^2]^2}, \tag{A3}$$

$$\delta\theta = \delta\chi = -\frac{\gamma\,\delta k_{\mathrm{res}}}{(k - k_{\mathrm{res}})^2 + \gamma^2}. \tag{A4}$$

For incoming electrons on resonance with the level, i.e., $|k - k_{\mathrm{res}}| \ll \gamma$, we obtain $\delta T \approx -2(k - k_{\mathrm{res}})\delta k_{\mathrm{res}}/\gamma^2$ and $\delta\theta = \delta\chi \approx -\delta k_{\mathrm{res}}/\gamma$, such that $\delta\theta, \delta\chi \gg \delta T$, and using $T \approx 1$ and $R \approx (k - k_{\mathrm{res}})^2/\gamma^2$, we find that $|\mathcal{I}S_{\mathrm{det,t}}| \gg |\mathcal{R}S_{\mathrm{det,r/t}}| \gg |\mathcal{I}S_{\mathrm{det,r}}|$. On the other hand, for off-resonant electrons $\delta T \approx -2\gamma^2\delta k_{\mathrm{res}}/(k - k_{\mathrm{res}})^3$ and $\delta\theta = \delta\chi \approx -\gamma\delta k_{\mathrm{res}}/(k - k_{\mathrm{res}})^2$, such that $\delta\theta, \delta\chi \gg \delta T$, and using $T \approx \gamma^2/(k - k_{\mathrm{res}})^2$ and $R \approx 1$, we find $|\mathcal{I}S_{\mathrm{det,r}}| \gg |\mathcal{R}S_{\mathrm{det,r/t}}| \gg |\mathcal{I}S_{\mathrm{det,t}}|$. When $|k - k_{\mathrm{res}}| \approx \gamma$, all response functions are of the same order.

A more realistic description for the quantum point contact (QPC) is achieved by considering a parabolic scattering potential $V_n(x) = V_n - kx^2/2$, where the offset V_n is the QPC barrier height when the dot is in the charge state $|n\rangle$. Here, we assume a quasiclassical description and consider the two limits of electrons with energy $E \gg V_n$ and $E \ll V_n$, respectively; see Fig. 4.

Using the Kemble formula [33], we obtain the transmission $T_n = 1/\{1 + \exp[-2\pi\sqrt{mL^2/8\hbar^2}(E - V_n)/\sqrt{V_n}]\}$, where we have chosen $V(\pm L/2) = 0$. For weak coupling $\delta V = V_1 - V_0 \ll V_0$, we obtain the shift (we define the energy scale $E_L = \hbar^2/2mL^2$)

$$\delta T = \frac{\pi}{4}\frac{E + V_0}{V_0}\,T_E R_E \frac{\delta V}{\sqrt{E_L V_0}}, \tag{A5}$$

which is suppressed exponentially for $E \gg V_0$ and $E \ll V_0$ due to an exponentially small reflection or transmission.

The change in phase at large energies $E \gg V_0$ is determined by the transmission phase accumulated in the region $[-L/2, L/2]$; within a quasiclassical description, this is given by ($\varepsilon \equiv E/V_n$)

$$\begin{aligned}\theta_n =& \frac{1}{\hbar}\int_{-L/2}^{L/2} dx\,\sqrt{2m[E - V_n(x)]}\\ =& \frac{1}{2}\sqrt{\frac{V_n}{E_L}}[\sqrt{\varepsilon} - (\varepsilon - 1)\log(\varepsilon - 1)^{1/2}\\ &+ (\varepsilon - 1)\log(1 + \sqrt{\varepsilon})].\end{aligned} \tag{A6}$$

Expanding this result for small δV, we obtain the change in phase $\delta\theta = \delta\chi$,

$$\delta\theta \approx -\frac{1}{3}\sqrt{\frac{V_0}{E}}\,\frac{\delta V}{\sqrt{E_L V_0}}. \tag{A7}$$

Given the exponential suppression of δT at large energies $E \gg V_0$, we find that $\delta T \ll |\delta\theta| = |\delta\chi|$, and for large transmission we have $|\mathcal{I}S_{\mathrm{det,t}}| \gg |\mathcal{R}S_{\mathrm{det,r/t}}| \gg |\mathcal{I}S_{\mathrm{det,r}}|$. In the opposite regime of small energies, $E \ll V_0$, we determine the change in phase (within quasiclassics) from the phase of the reflection amplitude,

$$\chi_n \approx \frac{2}{\hbar}\int_{-L/2}^{x_0} dx\sqrt{2m[E - V_n(x)]}, \tag{A8}$$

where the reversal point $x_0 < 0$ is characterized by $V(x_0) = E$. To leading order in δV, we find that

$$\delta\chi \approx -\frac{1}{3}\left(\frac{E}{V_0}\right)^{3/2}\frac{\delta V}{\sqrt{E_L V_0}}. \tag{A9}$$

Once more, it follows that $|\delta\theta|, |\delta\chi| \ll \delta T$ due to the exponential suppression of T, and the response functions respect the order $|\mathcal{R}S_{\mathrm{det,r}}| \gg |\mathcal{I}S_{\mathrm{det,r/t}}| \gg |\mathcal{R}S_{\mathrm{det,t}}|$. At intermediate energies, the response functions are of similar magnitude. Summarizing, we find that a scatterer with large transmission is characterized by the response functions satisfying $|\mathcal{R}S_{\mathrm{det,t}}| \gg |\mathcal{I}S_{\mathrm{det,r/t}}| \gg |\mathcal{R}S_{\mathrm{det,r}}|$ while at small transmission $|\mathcal{R}S_{\mathrm{det,r}}| \gg |\mathcal{I}S_{\mathrm{det,r/t}}| \gg |\mathcal{R}S_{\mathrm{det,t}}|$.

[1] G. B. Lesovik and R. Loosen, JETP Lett. **65**, 295 (1997).
[2] G. B. Lesovik, Phys. Usp. **41**, 145 (1998).
[3] R. Aguado and L. P. Kouwenhoven, Phys. Rev. Lett. **84**, 1986 (2000).
[4] K. V. Bayandin, A. V. Lebedev, and G. B. Lesovik, JETP **106**, 117 (2008).
[5] L. S. Levitov, H. W. Lee, and G. B. Lesovik, J. Math. Phys. **37**, 4845 (1996).
[6] D. A. Bagrets and Yu. V. Nazarov, Phys. Rev. B **67**, 085316 (2003).
[7] A. Di Lorenzo, G. Campagnano, and Y. V. Nazarov, Phys. Rev. B **73**, 125311 (2006).
[8] R. J. Glauber, Phys. Rev. Lett. **10**, 84 (1963).
[9] L. Mandel, Phys. Rev. **152**, 438 (1966).
[10] L. Mandel and E. Wolf, *Optical Coherence and Quantum Optics* (Cambridge University Press, Cambridge, 1995).
[11] A. Bednorz, C. Bruder, B. Reulet, and W. Belzig, Phys. Rev. Lett. **110**, 250404 (2013).
[12] G. B. Lesovik and I. A. Sadovskyy, Phys. Usp. **54**, 1007 (2011).
[13] D. Oehri, A. V. Lebedev, G. B. Lesovik, and G. Blatter, Phys. Rev. B **90**, 075312 (2014).
[14] J. von Neumann, *Mathematische Grundlagen der Quantentheorie* (Springer, Berlin, 1931).
[15] M. Nielsen and I. Chuang, *Quantum Computation and Quantum Information* (Cambridge University Press, Cambridge, 2000).
[16] M. Born, Z. Phys. **37**, 863 (1926).
[17] S. A. Gurvitz, Phys. Rev. B **56**, 15215 (1997).
[18] Y. Makhlin, G. Schön, and A. Shnirman, Phys. Rev. Lett. **85**, 4578 (2000).
[19] D. V. Averin and E. V. Sukhorukov, Phys. Rev. Lett. **95**, 126803 (2005).
[20] H. M. Wiseman and G. J. Milburn, *Quantum Measurement and Control* (Cambridge University Press, Cambridge, 2010).
[21] M. Field, C. G. Smith, M. Pepper, D. A. Ritchie, J. E. F. Frost, G. A. C. Jones, and D. G. Hasko, Phys. Rev. Lett. **70**, 1311 (1993); L. M. K. Vandersypen, J. M. Elzerman, R. N. Schouten, L. H. Willems van Beveren, R. Hanson, and L. P. Kouwenhoven, Appl. Phys. Lett. **85**, 4394 (2004); S. Gustavsson, R. Leturcq, B. Simovič, R. Schleser, T. Ihn, P. Studerus, K. Ensslin, D. C. Driscoll, and A. C. Gossard, Phys. Rev. Lett. **96**, 076605 (2006).
[22] G. Feve, A. Mahe, J.-M. Berroir, T. Kontos, B. Placais, D. C. Glattli, A. Cavanna, B. Etienne, and Y. Jin, Science **316**, 1169 (2007); J. Dubois, T. Jullien, F. Portier, P. Roche, A. Cavanna, Y. Jin, W. Wegscheider, P. Roulleau, and D. C. Glattli, Nature (London) **502**, 659 (2013).
[23] J. D. Fletcher, P. See, H. Howe, M. Pepper, S. P. Giblin, J. P. Griffiths, G. A. C. Jones, I. Farrer, D. A. Ritchie, T. J. B. M. Janssen, and M. Kataoka, Phys. Rev. Lett. **111**, 216807 (2013).
[24] E. Bocquillon, V. Freulon, J.-M. Berroir, P. Degiovanni, B. Plaçais, A. Cavanna, Y. Jin, and G. Fève, Science **339**, 1054 (2013).
[25] S. A. Gurvitz, Int. J. Mod. Phys. B **20**, 1363 (2006).
[26] A. V. Lebedev, G. B. Lesovik, and G. Blatter, Phys. Rev. B **72**, 245314 (2005).
[27] J. Keeling, I. Klich, and L. S. Levitov, Phys. Rev. Lett. **97**, 116403 (2006).
[28] C. Grenier, R. Hérvé, G. Fève, and P. Degiovanni, Mod. Phys. Lett. B **25**, 1053 (2011).
[29] R. Thalineau, A. D. Wieck, Ch. Bäuerle, and T. Meunier, arXiv:1403.7770.
[30] A. V. Lebedev and G. Blatter, Phys. Rev. B **77**, 035301 (2008).
[31] M. Tegmark, Nature (London) **448**, 23 (2007).
[32] *The Many-Worlds Interpretation of Quantum Mechanics*, edited by B. S. De Witt and N. Graham (Princeton University Press, Princeton, NJ, 1973).
[33] E. C. Kemble, Phys. Rev. **48**, 549 (1935).